BIOCHEMISTRY
including biophysical chemistry & molecular biology

Article

pubs.acs.org/biochemistry

Farnesyl Diphosphate Analogues with Aryl Moieties Are Efficient Alternate Substrates for Protein Farnesyltransferase

Thangaiah Subramanian,[†] June E. Pais,[§,∥] Suxia Liu,[†,⊥] Jerry M. Troutman,[†,@] Yuta Suzuki,[§] Karunai Leela Subramanian,[†] Carol A. Fierke,[§] Douglas A. Andres,[†] and H. Peter Spielmann*[,†,‡]

[†]Department of Molecular and Cellular Biochemistry and [‡]Department of Chemistry, Markey Cancer Center, and Kentucky Center for Structural Biology, University of Kentucky, Lexington, Kentucky 40536-0084, United States

[§]Departments of Chemistry and Biological Chemistry, University of Michigan, 930 North University, Ann Arbor, Michigan 48109-1055, United States

Supporting Information

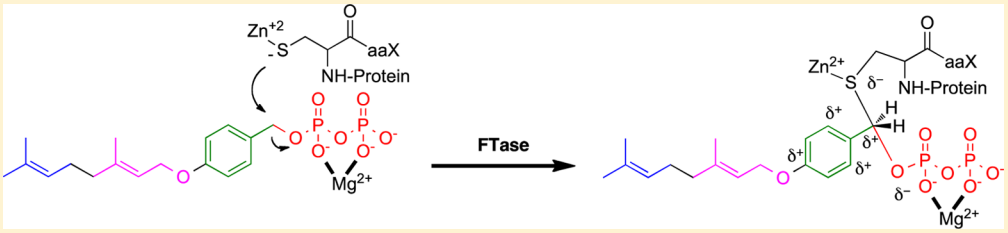

ABSTRACT: Farnesylation is an important post-translational modification essential for the proper localization and function of many proteins. Transfer of the farnesyl group from farnesyl diphosphate (FPP) to proteins is catalyzed by protein farnesyltransferase (FTase). We employed a library of FPP analogues with a range of aryl groups substituting for individual isoprene moieties to examine some of the structural and electronic properties of the transfer of an analogue to the peptide catalyzed by FTase. Analysis of steady-state kinetics for modification of peptide substrates revealed that the multiple-turnover activity depends on the analogue structure. Analogues in which the first isoprene is replaced with a benzyl group and an analogue in which each isoprene is replaced with an aryl group are good substrates. In sharp contrast with the steady-state reaction, the single-turnover rate constant for dansyl-GCVLS alkylation was found to be the same for all analogues, despite the increased chemical reactivity of the benzyl analogues and the increased steric bulk of other analogues. However, the single-turnover rate constant for alkylation does depend on the Ca_1a_2X peptide sequence. These results suggest that the isoprenoid transition-state conformation is preferred over the inactive E·FPP·Ca_1a_2X ternary complex conformation. Furthermore, these data suggest that the farnesyl binding site in the exit groove may be significantly more selective for the farnesyl diphosphate substrate than the active site binding pocket and therefore might be a useful site for the design of novel inhibitors.

Numerous membrane-associated proteins require post-translational farnesylation catalyzed by protein farnesyltransferase (FTase) for proper function. FTase catalyzes the transfer of a 15-carbon farnesyl group from farnesyl diphosphate **1** (FPP) to a conserved cysteine in the C-terminal Ca_1a_2X motif of a range of proteins, including the oncoprotein H-Ras (C refers to the cysteine, a to any aliphatic amino acid, and X to any amino acid).[1−8] The covalently attached isoprenoid increases the protein's hydrophobicity, promotes membrane localization, and enhances protein−protein interactions.[9−11] The clinical development of farnesyltransferase inhibitors (FTIs) as anticancer therapeutics has been hampered by alternative prenylation of some FTase substrates by the related prenyltransferase geranylgeranyl transferase type I (GGTase I) when FTase activity is limited.[12] This has spurred the development of alternative FTase-transferable lipids incapable of supporting normal prenyl group functions [prenyl function inhibitors (PFIs)].[13−16] Defining the isoprenoid chemical features that affect each step of the transferase reaction mechanism may provide useful insights for developing PFIs.[17]

The FTase kinetic mechanism is complex (Figure 1), and the enzyme rarely exists in the free, unbound form during the catalytic cycle. The FTase kinetic mechanism is thought to be functionally ordered, and efficient catalysis occurs when FPP first binds to the enzyme forming the enzyme·FPP complex (E·FPP) followed by Ca_1a_2X substrate association in which the active site zinc ion directly coordinates the cysteine thiolate to form a ternary complex (E·FPP·Ca_1a_2X) that is inactive based on the crystal structure.[18−21]

Models based on structural, mutagenesis, and computational studies in which a conformational rearrangement of the first two FPP isoprene units translocates the reactive isoprenoid C1 5.4 Å across the active site within reacting distance (2.4 Å) of the thiolate to form an active substrate conformation

Received: August 22, 2012
Published: September 18, 2012

   dx.doi.org/10.1021/bi3011362 | *Biochemistry* 2012, 51, 8307−8319

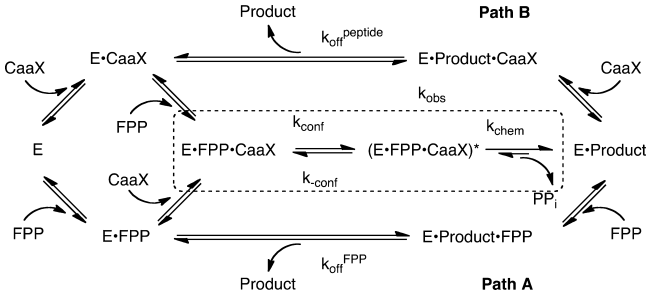

Figure 1. Basic kinetic pathway for FTase. Path A depicts FPP-stimulated product release and path B Ca_1a_2X peptide-stimulated product release. The dashed box encloses rate constants included in the observed single-turnover rate constant (k_{obs}).

(E·FPP·Ca_1a_2X*) have been proposed.[22−24] A variety of experiments suggest that the transfer of a farnesyl group to Ca_1a_2X thiol proceeds by a nucleophilic (S_N2, associative) mechanism with electrophilic (S_N1, dissociative) character, proceeding through a highly polar "exploded" transition state with considerable (C−1)−O bond cleavage and modest (C1)−S bond formation, partial positive charge on C−1, and partial negative charges on the zinc-coordinated sulfur and on the Mg^{2+}-coordinated diphosphate leaving group (Figure 2).[25−27]

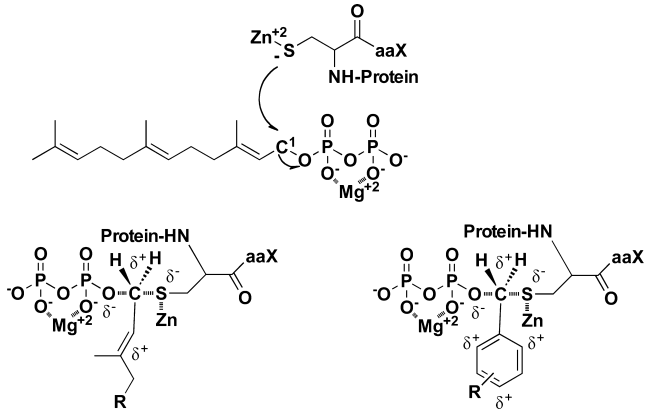

Figure 2. FTase-catalyzed peptide alkylation by FPP. The transition state is stabilized by positive charge delocalization on the allylic and benzylic systems of FPP and the analogues.

Recent computational studies suggest that the transition-state structure may depend on the structure of the peptide substrate.[28] The final step in the reaction cycle is product release, which is stimulated by binding of either a Ca_1a_2X peptide (path B) or FPP (path A) to form either the E·peptide or E·FPP complex.[29] The product release pathway depends on the sequence of the peptide.[22,23,30]

Because FPP is capable of binding to the free enzyme, the E·Ca_1a_2X complex, and the E·product complex, a better understanding of the binding interactions between the active site and FPP is needed and is of particular interest for the design of PFIs. FPP analogues have been employed to study the FTase mechanism and the interactions among the isoprenoid, enzymes, and the Ca_1a_2X peptide as well as the biological function of the post-translational modification. The reactivity of FPP analogues depends both on the isoprenoid structure and on the peptide substrate sequence.[15,31−33]

We report the synthesis and reactivity of FPP analogues with a range of steric demands and increased intrinsic chemical reactivity to investigate isoprenoid molecular features that contribute to substrate binding, recognition, and catalysis by FTase (Figure 3 and Table 1). The analogues vary with respect to the size and electronic properties of one, two, or all three isoprene groups. We used analogues that stabilize the carbocationic character of C1 to further examine the dissociative character of the transition state.

We have characterized FTase kinetic properties with these analogues and describe unexpected results with regard to their effect on catalysis. We measured single-turnover (STO) rate constants to examine the role of intrinsic chemical reactivity and steric bulk on the FPP conformational rearrangement and the chemical step [k_{obs} (Figure 1)]. Surprisingly, the STO rate constant is the same as that of FPP for all analogues tested, indicating that FTase-catalyzed peptide alkylation is very tolerant of the increased steric bulk in all three isoprene positions and that the rate of peptide alkylation is not limited by the chemical reactivity of the first isoprene in FPP. Within the series tested here, the hydrophobicity of the analogues does not limit the observed rate of thioether formation. However, the rate of peptide alkylation is dependent on the sequence of the C-terminal residue in the Ca_1a_2X motif. The steady-state data show that while some analogues are fairly good FTase substrates, others have $k_{cat}/K_M^{isoprenoid}$ values that are decreased up to 475-fold. These data indicate that a step subsequent to farnesylation, such as product dissociation, is sensitive to the structure of the farnesyl moiety.

EXPERIMENTAL PROCEDURES

Materials and Methods. The peptides TKCVIM, GCVLS, and dansylated GCVLS were synthesized and purified by high-pressure liquid chromatography to more than 90% purity by Sigma-Genosys (The Woodlands, TX), and the molecular masses of peptides were confirmed by electrospray mass spectrometry. 7-Diethylamino-3-({[(2-maleimidyl)ethyl]-amino}carbonyl)coumarin (MDCC) was purchased from Molecular Probes (Eugene, OR). Farnesyl diphosphate (FPP), purine nucleoside phosphorylase (PNPase), 7-methyl-guanosine (MEG), and inorganic pyrophosphatase from baker's yeast (PP_iase) were purchased from Sigma-Aldrich (St. Louis, MO). All other chemicals used were reagent grade.

All synthetic organic reactions except for resin preparation were performed in PTFE tubes using a Quest 210 apparatus manufactured by Argonaut Technologies. All RP-HPLC was performed on an Agilent 1100 HPLC system equipped with a microplate autosampler, a diode array, and a fluorescence detector. *N*-Dansyl-GCVLS was purchased from Peptidogenics (San Jose, CA). Spectrofluorometric analyses were performed in 96-well flat bottom, nonbinding surface, black polystyrene plates (Corning, excitation wavelength of 340 nm, emission wavelength of 505 nm with a 10 nm cutoff) with a SpectraMax GEMINI XPS fluorescence well-plate reader. Absorbance readings were determined using a Cary UV−vis spectrophotometer. All assays were performed at minimum in triplicate where the average values are reported with a one standard of deviation error. Reaction temperature refers to the external bath. All solvents and reagents were purchased from VWR (EM Science-Omnisolv high purity) and Aldrich respectively, and used as received. Merrifield-Cl resin was purchased from Argonaut Technologies. Synthetic products were purified by silica gel flash chromatography (EtOAc/hexane) unless otherwise noted. RP-HPLC purification of lipid diphosphates was conducted using a Varian Dynamax, 10 μm, 300 Å, C-18

dx.doi.org/10.1021/bi3011362 | *Biochemistry* 2012, 51, 8307−8319

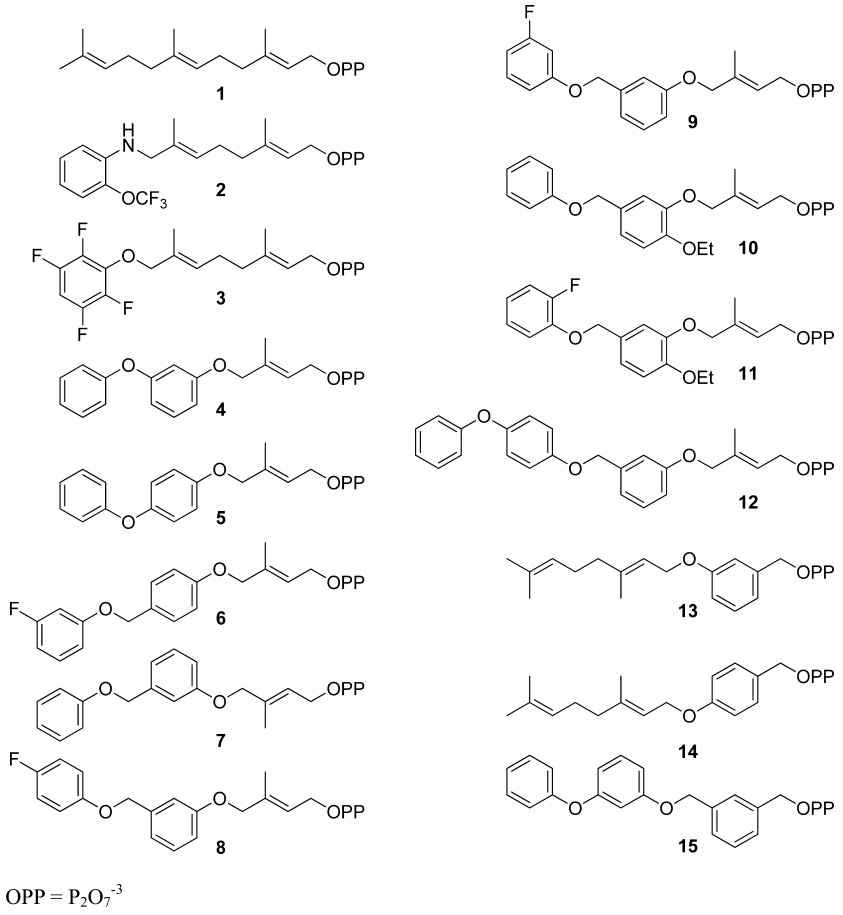

Figure 3. FPP and analogue structures.

Table 1. Kinetic Constants for the FTase-Catalyzed Reaction of FPP and Analogues with Ca_1a_2X Peptides

	steady-state kinetic parameters for alkylation of dns-GCVLS[a]			single-turnover rate constant k_{obs} (s^{-1})[b]		
isoprenoid	k_{cat} (s^{-1})	K_M (μM)	k_{cat}/K_M (μM^{-1} s^{-1})	GCVLS	TKCVIM	TKCVIF
1 (FPP)	0.29 ± 0.01	1.5 ± 0.2	192 ± 4	3.8	6.8	0.26
2	0.0021 ± 0.0001	0.49 ± 0.08	4.3 ± 0.5	4.1	5.8	ND[c]
3	0.43 ± 0.01	6.0 ± 0.7	72 ± 16	4.0	5.4	ND[c]
4	0.03 ± 0.002[d]	ND[c]	ND[c]	3.1	4.3	0.21
5	0.20 ± 0.01[d]	ND[c]	ND[c]	3.1	4.7	0.22
6	0.12 ± 0.01	5 ± 2	30 ± 10	3.7	5.0	ND[c]
7	0.017 ± 0.003	0.55 ± 0.09	30 ± 5	4.0	6.0	0.28
8	0.05 ± 0.01[d]	ND[c]	ND[c]	2.8	4.1	0.24
9	0.22 ± 0.04	5 ± 2	40 ± 20	3.5	5.0	ND[c]
10	>0.05[c]	>15[c]	1.4 ± 0.2	4.2	6.4	ND[c]
11	0.0013 ± 0.0001	3.1 ± 0.8	0.4 ± 0.01	4.0	6.3	ND[c]
12	ND[c,e]	ND[c]	ND[c]	3.8	6.2	0.29
13	0.0031 ± 0.0001	0.2 ± 0.1	15 ± 0	4.0	6.4	ND[c]
14	0.053 ± 0.002	0.5 ± 0.1	110 ± 20	3.9	6.0	ND[c]
15	0.29 ± 0.01	1.5 ± 0.2	300 ± 100	4.0	6.2	ND[c]

[a]Steady-state experiments were performed using dansylated peptides and measuring the time-dependent change in fluorescence.[44] Final solutions contained 25 nM FTase, 5 μM dns-GCVLS, varying concentrations (1−20 μM) of FPP/analogue, 50 mM Heppso (pH 7.8), 5 mM $MgCl_2$, and 2 mM TCEP. Assays were conducted at 25 °C. [b]Single-turnover rate constant, measured using an MDCC-PBP/PP_iase[58] assay on a stopped-flow fluorimeter. Measurements were repeated two or three times with a <10% error. Final solutions contained 400 nM FTase, 100 nM FPP/analogue, 25 μM peptide, 5 μM MDCC-PBP, 34 units/mL PP_iase, 50 mM Heppso (pH 7.8), 5 mM $MgCl_2$, and 2 mM TCEP. Assays were conducted at 25 °C. [c]Not determined. [d]Steady-state experiments were performed as described in footnote [a] except that k_{cat} was determined by varying the dns-GCVLS concentration (1−10 μM) at a saturating analogue concentration (20 μM). [e]The reaction was too slow to measure by the steady-state assay.

(10 mm × 250 mm) column and eluted with a gradient mobile phase and a flow rate of 4 mL/min (90% A from 0 to 3 min, 0% A from 3 to 18 min, 0% A from 18 to 20 min, and 90% A from 20 to 23 min) and monitored at 254 and 210 nm. ^{1}H NMR and ^{13}C NMR spectra of alcohols were obtained in $CDCl_3$ and ^{1}H and ^{31}P NMR spectra of diphosphates in D_2O with a Varian

dx.doi.org/10.1021/bi3011362 | Biochemistry 2012, 51, 8307−8319

Inova spectrometer operating at 400 MHz (^{1}H) and 161.8 MHz (^{31}P). Chemical shifts are reported in parts per million from the $CDCl_3$ internal peak at 7.27 ppm for ^{1}H (TSP, 0 ppm for ^{1}H; H_3PO_4 as an external reference, 0 ppm for ^{31}P). ESI-MS was performed at the University of Kentucky Mass Spectra Facility. Positive and negative ion electrospray ionization (ESI) mass spectra were recorded on a Thermo Finnigan LCQ instrument with sample introduction by direct infusion.

General Procedure for Mitsunobu Coupling (18a, 18b, 22a−c, 25a−g, 29a, and 29b). DEAD (40% in toluene, 1.2 equiv) was added dropwise to a stirred solution of alcohol (1 equiv), phenol (1.2 equiv), and Ph_3P (1.2 equiv) in THF at 0 °C and the mixture stirred for 1 h. After the reaction mixture had been allowed to warm to room temperature and stirred overnight, it was diluted with saturated $NaHCO_3$, concentrated, and extracted with CH_2Cl_2 (twice). The organic extracts were dried ($MgSO_4$), filtered, and concentrated. Silica gel column chromatography of the oily residue gave the desired compounds.

(E)-2-{[3-Methyl-4-(3-phenoxyphenoxy)but-2-en-1-yl]oxy}-tetrahydro-2H-pyran ***18a***. One gram of **16** gave 1.6 g of **18a** (84% yield): ^{1}H NMR ($CDCl_3$) δ 1.43−1.59 (m, 5H), 1.66−1.72 (m, 1H), 1.76 (s, 3H), 1.77−1.85 (m, 1H), 3.47−3.50 (m, 1H), 3.83−3.88 (m, 1H), 4.06−4.12 (m, 1H), 4.26−4.31 (m, 1H), 4.40 (s, 2H), 4.61 (t, J = 3.6 Hz, 1H), 4.75 (s, 2H), 5.74 (t, J = 6.4 Hz, 1H), 6.79−6.81 (m, 2H), 6.88−6.98 (m, 3H), 7.20−7.28 (m, 4H).

(E)-2-{[3-Methyl-4-(4-phenoxyphenoxy)but-2-en-1-yl]oxy}-tetrahydro-2H-pyran ***18b***. One gram of **16** gave 1.72 g of **18b** (91% yield): ^{1}H NMR ($CDCl_3$) δ 1.48−1.60 (m, 4H), 1.67−1.74 (m, 1H), 1.76 (s, 3H), 1.79−1.84 (m, 1H), 3.46−3.51 (m, 1H), 3.83−3.88 (m, 1H), 4.07−4.12 (m, 1H), 4.20−4.32 (m, 1H), 4.38 (s, 2H), 4.60 (t, J = 3.2 Hz, 1H), 5.72−5.75 (m, 1H), 6.84−6.95 (m, 6H), 6.99−7.03 (m, 1H).

(E)-3-({2-Methyl-4-[(tetrahydro-2H-pyran-2-yl)oxy]but-2-en-1-yl}oxy)benzaldehyde ***22a***. Five hundred milligrams of **16** gave 630 mg of **22a** (81% yield): ^{1}H NMR ($CDCl_3$) δ 1.46−1.60 (m, 4H), 1.60−1.72 (m, 1H), 1.76 (s, 3H), 1.77−1.81 (m, 1H), 3.45−3.51 (m, 1H), 3.82−3.87 (m, 1H), 4.06−4.11 (m, 1H), 4.26−4.31 (m, 1H), 4.45 (s, 2H), 4.60 (t, J = 6.8 Hz, 1H), 5.73−5.77 (m, 1H), 7.15−7.18 (m, 1H), 7.36−7.37 (m, 1H), 7.40−7.44 (m, 2H), 9.79 (s, 1H).

(E)-4-({2-Methyl-4-[(tetrahydro-2H-pyran-2-yl)oxy]but-2-en-1-yl}oxy)benzaldehyde ***22b***. Five hundred milligrams of **16** gave 619 mg of **22b** (69% yield): ^{1}H NMR ($CDCl_3$) δ 1.42−1.55 (m, 7H), 1.57−1.70 (m, 1H), 1.75 (s, 3H), 1.77−1.84 (m, 1H), 3.44−3.49 (m, 1H), 3.80−3.86 (m, 1H), 4.08−4.18 (m, 3H), 4.24−4.29 (m, 1H), 4.54 (s, 2H), 4.57 (t, J = 7.6 Hz, 1H), 5.71−5.75 (m, 1H), 6.91−7.00 (m, 1H), 7.34−7.38 (m, 2H), 9.79 (s, 1H).

(E)-4-Ethoxy-3-({2-methyl-4-[(tetrahydro-2H-pyran-2-yl)-oxy]but-2-en-1-yl}oxy)benzaldehyde ***22c***. Five hundred milligrams of **16** gave 690 mg of **22c** (85% yield): ^{1}H NMR ($CDCl_3$) δ 1.46−1.60 (m, 4H), 1.61−1.72 (m, 1H), 1.76 (s, 3H), 1.77−1.84 (m, 1H), 3.45−3.51 (m, 1H), 3.81−3.87 (m, 1H), 4.05−4.10 (m, 1H), 4.27−4.31 (m, 1H), 4.47 (s, 2H), 4.59 (t, J = 3.6 Hz, 1H), 5.72−5.76 (m, 1H), 6.98 (d, J = 8.8 Hz, 2H), 7.79 (d, J = 8.8 Hz, 2H), 9.84 (s, 1H).

(E)-2-[(4-{4-[(3-Fluorophenoxy)methyl]phenoxy}-3-methylbut-2-en-1-yl)oxy]tetrahydro-2H-pyran ***25a***. One hundred milligrams of **23b** gave 104 mg of **25a** (82.5% yield): ^{1}H NMR ($CDCl_3$) δ 1.40−1.70 (m, 5H), 1.77−1.81 (m, 1H), 1.78 (s, 3H), 3.47−3.50 (m, 1H), 3.83−8.88 (m, 1H), 4.08−4.12 (m, 1H), 4.30 (m, 1H), 4.41 (s, 2H), 4.61 (t, J = 3.6 Hz, 2H), 4.92 (s, 2H), 5.73 (t, J = 6.0 Hz, 1H), 6.90 (d, J = 8.8 Hz, 2H), 6.95−7.10 (m, 5H), 7.15−7.20 (2H).

(E)-2-({3-Methyl-4-[3-(phenoxymethyl)phenoxy]but-2-en-1-yl}oxy)tetrahydro-2H-pyran ***25b***. One hundred milligrams of **23a** gave 117 mg of **25b** (87% yield): ^{1}H NMR ($CDCl_3$) δ 1.49−1.59 (m, 5H), 1.72 (s, 3H), 1.77−1.85 (m, 1H), 3.46−3.52 (m, 1H), 3.83−3.88 (m, 1H), 4.06−4.12 (m, 1H), 4.26−4.31 (m, 1H), 4.40 (s, 2H), 4.60 (t, J = 4.0 Hz, 1H), 5.00 (s, 2H), 5.72−5.75 (m, 1H), 6.79−6.85 (m, 1H), 6.90−6.98 (m, 4H), 7.20−7.28 (m, 4H).

(E)-2-[(4-{3-[(4-Fluorophenoxy)methyl]phenoxy}-3-methylbut-2-en-1-yl)oxy]tetrahydro-2H-pyran ***25c***. One hundred milligrams of **23a** gave 117 mg of **25c** (82% yield): ^{1}H NMR ($CDCl_3$) δ 1.48−1.69 (m, 5H), 1.77−1.81 (m, 1H), 1.78 (s, 3H), 3.47−3.50 (m, 1H), 3.83−3.88 (m, 1H), 4.08−4.11 (m, 1H), 4.28 (dd, J = 6.4, 12.4 Hz, 1H), 4.41 (s, 2H), 4.60 (t, J = 3.6 Hz, 2H), 4.93 (s, 2H), 5.73 (t, J = 6.0 Hz, 1H), 6.90 (d, J = 8.8 Hz, 2H), 7.14−7.18 (m, 3H), 7.30 (d, J = 8.8 Hz, 2H).

(E)-2-[(4-{3-[(3-Fluorophenoxy)methyl]phenoxy}-3-methylbut-2-en-1-yl)oxy]tetrahydro-2H-pyran ***25d***. One hundred milligrams of **23a** gave 117 mg of **25d** (81% yield): ^{1}H NMR ($CDCl_3$) δ 1.48−1.69 (m, 5H), 1.77−1.81 (m, 1H), 1.76 (s, 3H), 3.46−3.51 (m, 1H), 3.83−3.88 (m, 1H), 4.06−4.11 (m, 1H), 4.26−4.31 (m, 1H), 4.40 (s, 2H), 4.60 (t, J = 4.0 Hz, 2H), 4.97 (s, 2H), 5.72−5.75 (m, 1H), 6.72−6.75 (m, 1H), 6.83−6.97 (m, 6H), 7.24−7.27 (m, 1H).

(E)-2-({4-[2-Ethoxy-5-(phenoxymethyl)phenoxy]-3-methylbut-2-en-1-yl}oxy)tetrahydro-2H-pyran ***25e***. One hundred milligrams of **23c** gave 77 mg of **25e** (77% yield): ^{1}H NMR ($CDCl_3$) δ 1.41 (t, J = 7.2 Hz, 3H), 1.48−1.69 (m, 5H), 1.76 (s, 3H), 1.77−1.81 (m, 1H), 3.46−3.51 (m, 1H), 3.82−3.88 (m, 1H), 4.06−4.11 (m, 1H), 4.26 (dd, J = 6.4, 12.4 Hz, 1H), 4.46 (s, 2H), 4.58 (t, J = 2.8 Hz, 1H), 4.93 (s, 2H), 5.70−5.73 (m, 1H), 6.84−6.96 (m, 6H), 7.23−7.28 (m, 2H).

(E)-2-[(4-{2-Ethoxy-5-[(2-fluorophenoxy)methyl]phenoxy}-3-methylbut-2-en-1-yl)oxy]tetrahydro-2H-pyran ***25f***. One hundred milligrams of **23c** gave 120 mg of **25f** (80% yield): ^{1}H NMR ($CDCl_3$) δ 1.42 (t, J = 7.2 Hz, 3H), 1.48−1.69 (m, 5H), 1.76 (s, 3H), 1.77−1.81 (m, 1H), 3.46 (dd, J = 4.4, 10.4 Hz, 1H), 3.82−3.87 (m, 1H), 4.05−4.12 (m, 3H), 4.25 (dd, J = 6, 12.4 Hz, 1H), 4.46 (s, 2H), 4.58 (t, J = 2.4 Hz, 1H), 5.02 (s, 2H), 5.71 (t, J = 7.6 Hz, 1H), 6.95−7.10 (m, 4H), 6.82−6.90 (m, 3H).

(E)-2-[(3-Methyl-4-{3-[(4-phenoxyphenoxy)methyl]-phenoxy}but-2-en-1-yl)oxy]tetrahydro-2H-pyran ***25g***. One hundred milligrams of **23c** gave 123 mg of **25g** (78% yield): ^{1}H NMR ($CDCl_3$) δ 1.45−1.60 (m, 6H), 1.65−1.75 (m, 2H), 1.78 (s, 3H), 1.79−1.82 (m, 1H), 3.44−3.50 (m, 1H), 3.82−3.90 (m, 1H), 4.06−4.12 (m, 1H), 4.26−4.34 (m, 1H), 4.41 (s, 2H), 4.58−4.62 (m, 1H), 4.98 (s, 2H), 5.72−5.78 (m, 1H), 6.78−6.80 (m, 1H), 6.83−7.06 (m, 8H), 7.20−7.30 (m, 4H).

(E)-3-[(3,7-Dimethylocta-2,6-dien-1-yl)oxy]benzaldehyde ***29a***. One gram of geraniol gave 1.6 g of **29a** (95% yield): ^{1}H NMR ($CDCl_3$) δ 1.57 (s, 3H), 1.64 (s, 3H), 1.72 (s, 3H), 2.03−2.11 (m, 4H), 4.56 (s, 2H), 4.58 (s, 2H), 5.04−5.08 (m, 1H), 5.44−5.48 (m, 1H), 7.15−7.18 (m, 1H), 7.37−7.42 (m, 3H), 9.94 (s, 1H).

(E)-4-[(3,7-Dimethylocta-2,6-dien-1-yl)oxy]benzaldehyde ***29b***. One gram of geraniol gave 1.6 g of **29b** (78% yield): ^{1}H NMR ($CDCl_3$) δ 1.57 (s, 3H), 1.64 (s, 3H), 1.72 (s, 3H), 2.02−2.14 (m, 4H), 4.60 (d, J = 6.8 Hz, 2H), 5.03−5.06 (m,

1H), 5.43−5.46 (m, 1H), 6.97 (d, J = 8.8 Hz, 2H), 7.80 (d, J = 8.8 Hz, 2H), 9.85 (s, 1H).

General Procedure for THP Ether Removal. THP ether and 5% (w/v) PPTS were stirred in dry MeOH overnight. The reaction mixture was evaporated, taken up in ethyl acetate, washed with saturated $NaHCO_3$ and brine, dried ($MgSO_4$), filtered, and evaporated. Chromatographic purification of the residue gave alcohol in quantitative yield.

(E)-3-Methyl-4-(3-phenoxyphenoxy)but-2-en-1-ol ***19a:*** ^{1}H NMR ($CDCl_3$) δ 1.75 (s, 3H), 4.25 (d, J = 6.8 Hz, 2H), 4.40 (s, 2H), 5.72−5.77 (m, 1H), 6.55−6.60 (m, 2H), 6.64 (ddd, J = 0.8, 2.4, 8.4 Hz, 1H), 7.00−7.03 (m, 2H), 7.08−7.12 (m, 1H), 7.18−7.22 (m, 1H), 7.30−7.35 (m, 2H).

(E)-3-Methyl-4-(4-phenoxyphenoxy)but-2-en-1-ol ***19b:*** ^{1}H NMR ($CDCl_3$) δ 1.75 (s, 3H), 4.22 (d, J = 6.8 Hz, 2H), 4.36 (s, 2H), 5.72−5.77 (m, 1H), 6.55−6.60 (m, 2H), 6.64 (ddd, J = 0.8, 2.4, 8.4 Hz, 1H), 6.85−6.90 (m, 4H), 7.00−7.03 (m, 1H), 7.08−7.12 (m, 1H), 7.30−7.35 (m, 2H).

(E)-4-{4-[(3-Fluorophenoxy)methyl]phenoxy}-3-methylbut-2-en-1-ol ***26a:*** ^{1}H NMR ($CDCl_3$) δ 1.78 (s, 3H), 4.20 (d, J = 5.6 Hz, 2H), 4.42 (s, 2H), 5.05 (s, 2H), 5.78−5.80 (m, 1H), 6.81−6.90 (m, 1H), 6.90−7.10 (m, 5H), 7.28−7.35 (m, 3H).

(E)-3-Methyl-4-[3-(phenoxymethyl)phenoxy]but-2-en-1-ol ***26b:*** ^{1}H NMR ($CDCl_3$) δ 1.78 (s, 3H), 4.20 (d, J = 5.6 Hz, 2H), 4.42 (s, 2H), 5.05 (s, 2H), 5.78−5.80 (m, 1H), 6.81−6.90 (m, 1H), 6.90−7.10 (m, 5H), 7.28−7.35 (m, 3H).

(E)-4-{3-[(4-Fluorophenoxy)methyl]phenoxy}-3-methylbut-2-en-1-ol ***26c:*** ^{1}H NMR ($CDCl_3$) δ 1.54 (s, 3H), 1.76 (brs, 1H), 4.22 (d, J = 5.6 Hz, 2H), 4.40 (s, 2H), 4.97 (s, 2H), 5.74−5.79 (m, 1H), 6.83−7.00 (m, 7H), 7.23−7.27 (m, 1H).

(E)-4-{3-[(3-Fluorophenoxy)methyl]phenoxy}-3-methylbut-2-en-1-ol ***26d:*** ^{1}H NMR ($CDCl_3$) δ 1.42 (t, J = 7.2 Hz, 3H), 1.77 (s, 3H), 4.07 (q, J = 6.8, 14 Hz, 2H), 4.21 (t, J = 5.6 Hz, 2H), 4.45 (s, 2H), 4.94 (s, 2H), 5.74−5.78 (m, 1H), 6.83−6.96 (m, 6H), 7.23−7.28 (m, 2H).

(E)-4-[2-Ethoxy-5-(phenoxymethyl)phenoxy]-3-methylbut-2-en-1-ol ***26e:*** ^{1}H NMR ($CDCl_3$) δ 1.41 (t, J = 7.2 Hz, 3H), 1.76 (s, 3H), 4.07(q, J = 6.8, 14 Hz, 2H), 4.20 (t, J = 6.0 Hz, 2H), 4.45 (s, 2H), 5.02 (s, 2H), 5.75−5.78 (m, 1H), 6.82−6.91 (m, 3H), 6.95−7.08 (m, 4H).

(E)-4-{2-Ethoxy-5-[(2-fluorophenoxy)methyl]phenoxy}-3-methylbut-2-en-1-ol ***26f:*** ^{1}H NMR ($CDCl_3$) δ 1.40 (t, J = 7.2 Hz, 3H), 1.80 (s, 3H), 4.0 (q, J = 6.8, 14 Hz, 2H), 4.10 (t, J = 6.0 Hz, 2H), 4.40 (s, 2H), 5.00 (s, 2H), 5.78 (t, J = 14 Hz, 1H), 6.80−7.05 (m, 7H).

(E)-3-Methyl-4-{3-[(4-phenoxyphenoxy)methyl]phenoxy}-but-2-en-1-ol ***26g:*** ^{1}H NMR ($CDCl_3$) δ 1.76 (s, 3H), 4.22 (t, J = 5.6 Hz, 2H), 4.42 (s, 2H), 5.00 (s, 2H), 5.75−5.80 (m, 1H), 6.84−6.87 (m, 1H), 6.91−7.04 (m, 9H), 7.23−7.29 (m, 3H).

{3-[(3-Phenoxyphenoxy)methyl]phenyl}methanol ***36:*** ^{1}H NMR ($CDCl_3$) δ 4.70 (s, 2H), 5.02 (s, 2H), 6.90−6.96 (m, 5H), 7.00−7.04 (m, 1H), 7.23−7.25 (m, 2H), 7.36−7.42 (m, 4H).

General Procedure for Aldehyde Reduction. $NaBH_4$ (2 equiv) was added to aldehyde (1 equiv) in EtOH at 0 °C and the mixture stirred for 3−6 h. The mixture was diluted with water and extracted with CH_2Cl_2 (twice). The organic extracts were dried ($MgSO_4$), filtered, and evaporated. The silica gel column chromatographic purification of the oily residue gave the alcohol in quantitative yield.

(E)-[3-({4-[(Tetrahydro-2H-pyran-2-yl)oxy]but-2-en-1-yl}-oxy)phenyl]methanol ***23a:*** ^{1}H NMR ($CDCl_3$) δ 1.48−1.57 (m, 5H), 1.62−1.72 (m, 2H), 1.76 (s, 3H), 1.79−1.84 (m, 1H), 3.46−3.51 (m, 1H), 3.82−3.87 (m, 1H), 4.06−4.11 (m, 1H), 4.26−4.31 (m, 1H), 4.41 (s, 2H), 4.59 (t, J = 3.6 Hz, 1H), 4.64 (d, J = 4.4 Hz, 2H), 5.72−5.75 (m, 1H), 6.80−6.92 (m, 1H), 6.90−6.92 (m, 2H), 7.21−7.25 (m, 1H).

(E)-[4-({2-Methyl-4-[(tetrahydro-2H-pyran-2-yl)oxy]but-2-en-1-yl}oxy)phenyl]methanol ***23b:*** ^{1}H NMR ($CDCl_3$) δ 1.40−1.44 (m, 3H), 1.48−1.56 (m, 5H), 1.65−1.71 (m, 1H), 1.76 (s, 3H), 3.45−3.48 (m, 1H), 3.82−3.87 (m, 1H), 4.02−4.13 (m, 2H), 4.24−4.28 (m, 1H), 4.45 (s, 2H), 4.56−4.58 (m, 3H), 5.71 (t, J = 7.2 Hz, 1H), 6.79−6.90 (m, 4H).

(E)-[4-Ethoxy-3-({2-methyl-4-[(tetrahydro-2H-pyran-2-yl)-oxy]but-2-en-1-yl}oxy)phenyl]methanol ***23c:*** ^{1}H NMR ($CDCl_3$) δ 1.48−1.56 (m, 5H), 1.68−1.73 (m, 2H), 1.76 (s, 3H), 1.77−1.85 (m, 1H), 3.46−3.51 (m, 1H), 3.83−3.88 (m, 1H), 4.06−4.12 (m, 1H), 4.27−4.32 (m, 1H), 4.40 (s, 2H), 4.59−4.61 (m, 3H), 5.72−5.75 (m, 1H), 6.87 (d, J = 8.8 Hz, 2H), 7.25 (d, J = 8.8 Hz, 2H).

(E)-{3-[(3,7-Dimethylocta-2,6-dien-1-yl)oxy]phenyl}-methanol ***30a:*** ^{1}H NMR ($CDCl_3$) δ 1.58 (s, 3H), 1.65 (s, 3H), 1.71 (s, 3H), 2.05−2.09 (m, 4H), 4.52 (d, J = 6.4 Hz, 2H), 4.64 (s, 2H), 5.07 (t, J = 6.8 Hz, 1H), 5.46 (t, J = 8.0 Hz, 1H), 6.81−6.83 (m, 1H), 6.89−6.92 (m, 2H), 7.22−7.26 (m, 1H).

(E)-{4-[(3,7-Dimethylocta-2,6-dien-1-yl)oxy]phenyl}-methanol ***30b:*** ^{1}H NMR ($CDCl_3$) δ 1.58 (s, 3H), 1.65 (s, 3H), 1.71 (s, 3H), 2.04−2.11 (m, 4H), 4.51 (d, J = 7.2 Hz, 2H), 4.59 (d, J = 6.0 Hz, 2H), 5.05−5.08 (m, 1H), 5.44−5.48 (m, 1H), 6.88 (d, J = 8.8 Hz, 2H), 7.26 (d, J = 8.8 Hz, 2H).

General Procedure for Diphosphate Synthesis. Ph_3PCl_2 (2 equiv) in dry CH_3CN was added dropwise to a cooled (0 °C) solution of the alcohol (1 equiv) in CH_3CN (5 mL) and the mixture stirred for 2 h. The reaction mixture was concentrated and filtered through a pad of silica gel. The chlorides were sufficiently pure to proceed to the next step. $[(n\text{-}Bu)_4N]_3HP_2O_7$ (5 equiv) in CH_3CN was then added to the solution of chloride in CH_3CN at 0 °C, and the solution was allowed to warm to room temperature and stirred overnight. The reaction mixture was concentrated and washed with Et_2O. The organic extracts were discarded, and the residue was suspended in 4 mL of ion exchange buffer [25 mM NH_4HCO_3 in 2% (v/v) i-PrOH/water]. The resultant white solution was loaded onto a pre-equilibrated 6 cm × 50 cm column of Dowex AG 50W-X8 (100−200 mesh) cation exchange resin (NH_4^+ form). The flask was washed with buffer (2 × 2 mL) and loaded onto the column before elution with 150 mL of ion exchange buffer. The eluent was lyophilized to yield a white solid. This solid was dissolved in a 25 mM solution of NH_4HCO_3 buffer (4 mL), purified by RP-HPLC (retention time of ∼7 min), and lyophilized to give the diphosphate as a white powder.

(2E,6E)-3,7-Dimethyl-8-(2,3,5,6-tetrafluorophenoxy)octa-2,6-dien-1-diphosphate ***3*** *(26% in two steps from the Mitsunobu reaction product):*[14] ^{1}H NMR (D_2O) δ 1.50 (s, 3H), 1.60 (s, 3H), 1.83−1.87 (m, 2H), 1.98−2.04 (m, 2H), 4.27 (t, J = 6.4 Hz, 2H), 4.49 (s, 2H), 5.23 (t, J = 7.6 Hz, 1H), 5.36 (t, J = 6.8 Hz, 1H), 6.87−6.95 (m, 1H); ^{31}P NMR (D_2O) δ −5.90 (d, J = 22 Hz, 1P), −9.49 (d, J = 22 Hz, 1P); LRMS(EI) ($M^+ - H^+$) 477, (M^+) 478

(E)-3-Methyl-4-(3-phenoxyphenoxy)but-2-en-1-diphosphate ***4.*** One hundred milligrams of **19a** gave 42.7 mg of **4** (23% yield): ^{1}H NMR (D_2O) δ 1.63 (s, 3H), 4.40 (s, 2H), 4.64 (s, 2H), 5.63−5.69 (m, 1H), 6.85−6.89 (m, 1H), 6.97−7.01 (m, 1H), 7.21−7.25 (m, 2H); ^{31}P NMR (D_2O) δ −9.7 (d, J = 22 Hz, 1P), 8.76 (d, J = 22 Hz, 1P); LRMS(EI) ($M^+ - H^+$) 429, (M^+) 430.

dx.doi.org/10.1021/bi3011362 | *Biochemistry* 2012, 51, 8307−8319

(E)-3-Methyl-4-(4-phenoxyphenoxy)but-2-en-1-diphosphate ***5***. One hundred milligrams of **19b** gave 53 mg of **5** (28% yield): ^{1}H NMR (D_2O) δ 1.58 (s, 3H), 4.35 (bs, 2H), 4.62 (s, 2H), 5.58 (t, J = 5.6 Hz, 1H), 6.50−6.54 (m, 2H), 6.65 (ddd, J = 0.8, 2.4, 8.4 Hz, 1H), 6.91−6.94 (m, 2H), 7.03−7.07 (m, 1H), 7.14−7.18 (m, 1H), 7.25−7.30 (m, 2H); ^{31}P NMR (D_2O) δ −9.7 (d, J = 20.8 Hz, 1P), −8.51 (d, J = 20.8 Hz, 1P); LRMS(EI) ($M^+ - H^+$) 429, (M^+) 430.

(E)-4-{4-[(3-Fluorophenoxy)methyl]phenoxy}-3-methylbut-2-en-1-diphosphate ***6***. Fifty milligrams of **26a** gave 20 mg of **6** (22% yield): ^{1}H NMR (D_2O) δ 1.59 (s, 3H), 4.35 (t, J = 7.2 Hz, 2H), 4.40 (s, 2H), 5.00 (s, 2H), 5.61 (t, J = 6.8 Hz, 1H), 6.83−7.00 (m, 6H), 7.17−7.21 (m, 3H); ^{31}P NMR (D_2O) δ −9.35 (d, J = 22.0 Hz, 1P), −9.82 (d, J = 22.0 Hz, 1P); LRMS(EI) ($M^+ - H^+$) 429, (M^+) 430.

(E)-3-Methyl-4-[3-(phenoxymethyl)phenoxy]but-2-en-1-diphosphate ***7***. Fifty milligrams of **26b** gave 24 mg of **7** (28% yield): ^{1}H NMR (D_2O) δ 1.58 (s, 3H), 4.33 (t, J = 5.6 Hz, 2H), 4.35 (s, 2H), 4.94 (s, 2H), 5.61 (t, J = 6.4 Hz, 1H), 6.80−6.92 (m, 2H), 7.15−7.19 (m, 2H); ^{31}P NMR (D_2O) δ −5.8 (d, J = 20.0 Hz, 1P), −9.39 (d, J = 20.0 Hz, 1P); LRMS(EI) ($M^+ - H^+$) 443, (M^+) 444.

(E)-4-{3-[(4-Fluorophenoxy)methyl]phenoxy}-3-methylbut-2-en-1-diphosphate ***8***. Fifty milligrams of **26c** gave 21 mg of **8** (25% yield): ^{1}H NMR (D_2O) δ 1.60 (s, 3H), 4.37 (t, J = 6.8 Hz, 1H), 4.40 (s, 2H), 5.0 (s, 2H), 5.63 (t, J = 7.2 Hz, 1H), 6.84−7.14 (m, 7H), 7.18−7.22 (m, 2H); ^{31}P NMR (D_2O) δ −7.48 (d, J = 20.0 Hz, 1P), −9.55 (d, J = 20.0 Hz, 1P); LRMS(EI) ($M^+ - H^+$) 461, (M^+) 462.

(E)-4-{3-[(3-Fluorophenoxy)methyl]phenoxy}-3-methylbut-2-en-1-diphosphate ***9***. Fifty milligrams of **26d** gave 22 mg of **9** (28% yield): ^{1}H NMR (D_2O) δ 1.58 (s, 3H), 4.33−4.35 (m, 4H), 4.94 (s, 2H), 5.61 (t, J = 6.0 Hz, 1H), 6.80−6.92 (m, 5H), 7.15−7.19 (m, 3H); ^{31}P NMR (D_2O) δ −5.74 (d, J = 19.6 Hz, 1P), −9.40 (d, J = 19.6 Hz, 1P); LRMS(EI) ($M^+ - H^+$) 461, (M^+) 462.

(E)-4-[2-Ethoxy-5-(phenoxymethyl)phenoxy]-3-methylbut-2-en-1-diphosphate ***10***. Fifty milligrams of **26e** gave 31 mg of **10** (36% yield): ^{1}H NMR (D_2O) δ 1.15 (t, J = 7.2 Hz, 3H), 1.56 (s, 3H), 3.92 (q, J = 6.8, 14 Hz, 2H), 4.33 (t, J = 6.4 Hz, 2H), 4.37 (s, 2H), 4.86 (s, 2H), 5.56 (t, J = 6.0 Hz, 1H), 6.82−6.93 (m, 6H), 7.13−7.17 (m, 2H); ^{31}P NMR (D_2O) δ −7.03 (d, J = 19.5 Hz, 1P), −9.39 (d, J = 19.5 Hz, 1P); LRMS(EI) ($M^+ - H^+$) 487, (M^+) 488.

(E)-4-{2-Ethoxy-5-[(2-fluorophenoxy)methyl]phenoxy}-3-methylbut-2-en-1-diphosphate ***11***. Fifty milligrams of **26f** gave 18 mg of **11** (22% yield): ^{1}H NMR (D_2O) δ 1.16 (t, J = 7.2 Hz, 3H), 1.57 (s, 3H), 3.91 (q, J = 6.8, 14.0 Hz, 3H), 4.33 (t, J = 6.4 Hz, 2H), 4.37 (s, 2H), 4.86 (s, 2H), 5.56 (t, J = 6.4 Hz, 1H), 6.82−6.85 (m, 5H), 6.93 (s, 1H), 7.13−7.17 (m, 2H); ^{31}P NMR (D_2O) δ −7.03 (brs, 1P), −9.59 (brs, 1P); LRMS(EI) ($M^+ - H^+$) 505, (M^+) 506.

(E)-3-Methyl-4-{3-[(4-phenoxyphenoxy)methyl]phenoxy}-but-2-en-1-diphosphate ***12***. Fifty milligrams of **26g** gave 21 mg of **12** (26% yield): ^{1}H NMR ($CDCl_3$) δ 1.20 (t, J = 7.6 Hz, 3H), 1.60 (s, 3H), 3.93 (q, J = 7.2, 14 Hz, 2H), 4.37 (t, J = 6.4 Hz, 2H), 4.40 (s, 2H), 4.94 (s, 2H), 5.59 (t, J = 6.0 Hz, 1H), 6.80−6.84 (m, 3H), 6.92−7.10 (m, 4H); ^{31}P NMR (D_2O) δ −9.59 (brs, 1P), −7.81 (brs, 1P); LRMS(EI) ($M^+ - H^+$) 535, (M^+) 536.

(E)-{3-[(3,7-Dimethylocta-2,6-dien-1-yl)oxy]phenyl}-methanyldiphosphate ***13***. One hundred milligrams of **30a** gave 34.5 mg of **13** (19% yield): ^{1}H NMR (D_2O) δ 1.42 (s, 3H), 1.47 (s, 3H), 1.93−1.99 (m, 4H), 4.47 (d, J = 6.8 Hz, 2H), 5.31 (t, J = 6.0 Hz, 1H), 4.97 (t, J = 6.4 Hz, 1H), 6.80 (d, J = 8.8 Hz, 2H), 7.26 (d, J = 8.8 Hz, 2H); ^{31}P NMR (D_2O) δ −10.02 (d, J = 22.0 Hz, 1P), −8.00 (d, J = 22.0 Hz, 1P); LRMS(EI) ($M^+ - H^+$) 419, (M^+) 420.

(E)-{4-[(3,7-Dimethylocta-2,6-dien-1-yl)oxy]phenyl}-methanyldiphosphate ***14***. One hundred milligrams of **30b** gave 32.0 mg of **14** (18% yield): ^{1}H NMR (D_2O) δ 1.42 (s, 3H), 1.47 (s, 3H), 1.56 (s, 3H), 1.94−2.02 (m, 4H), 4.49 (d, J = 8.0 Hz, 2H), 4.80 (d, J = 6.0 Hz, 2H), 4.98 (t, J = 7.2 Hz, 1H), 5.33 (t, J = 6.0 Hz, 1H), 6.76−6.78 (m, 1H), 6.94−6.96 (m, 2H), 7.16−7.20 (m, 1H); ^{31}P NMR (D_2O) δ −9.78 (d, J = 22.0 Hz, 1P), −5.93 (d, J = 22.0 Hz, 1P); LRMS(EI) ($M^+ - H^+$) 419, (M^+) 420.

{3-[(3-Phenoxyphenoxy)methyl]phenyl}-methanyldiphosphate ***15***. Fifty milligrams of **36** gave 23 mg of **15** (27% yield): ^{1}H NMR (D_2O) δ 1.73 (s, 3H), 4.97 (s, 2H), 5.82 (d, J = 6.4 Hz, 2H), 4.97 (s, 2H), 6.51−6.53 (m, 2H), 6.68 (dd, J = 2.0, 9.6 Hz, 2H), 6.87−6.89 (m, 2H), 7.05 (t, J = 7.6 Hz, 1H), 7.15−7.34 (m, 7H); ^{31}P NMR (D_2O) δ −7.10 (d, J = 22 Hz, 1P), 9.87 (d, J = 22 Hz, 1P); LRMS(EI) ($M^+ - H^+$) 465, (M^+) 466.

2-({3-[(3-Phenoxyphenoxy)methyl]benzyl}oxy)tetrahydro-2H-pyran ***35***. To the cooled 0 °C solution of *m*-hydroxyphenol **33** (500 mg, 2.68 mmol) in dry DMF was added 60% sodium hydride in mineral oil (129 mg, 3.2 mmol). The resultant solution was stirred for 1 h at 0 °C and for 2 h at room temperature. 2-{[3-(Chloromethyl)benzyl]oxy}tetrahydro-2*H*-pyran (645 mg, 2.68 mmol) was added dropwise and the mixture stirred overnight. The reaction was quenched with water, the mixture extracted with methylene chloride, and the organic phase washed with water (thrice). The combined organic extracts were washed with brine, dried over $MgSO_4$, concentrated, and purified by silica gel column chromatography (hexanes, ethyl acetate) to yield oily residue **35** (980 mg, 93%): ^{1}H NMR ($CDCl_3$) δ 1.47−1.81 (m, 2H), 1.80−1.88 (m, 1H), 3.49−3.55 (m, 1H), 3.86−3.92 (m, 1H), 4.49 (d, J = 12.0 Hz, 2H), 4.68 (t, J = 3.6 Hz, 1H), 4.78 (d, J = 12.4 Hz, 2H), 5.00 (s, 2H), 5.57−6.62 (m, 2H), 6.70 (dd, J = 2.4, 8.4 Hz, 1H), 6.98−7.01 (m, 2H), 7.06−7.10 (m, 1H), 7.17−7.28 (m, 1H), 7.29−7.39 (m, 6H).

Preparation of MDCC-PBP. The purification and labeling of the His_6-tagged A197C phosphate binding protein (PBP) with the coumarin fluorophore MDCC were performed as described previously.[27,34] The final MDCC-labeled PBP was dialyzed against 50 mM Hepes (pH 7.8), 2 mM TCEP, 0.5 unit/mL purine nucleoside phosphorylase, and 15 mM 7-methylguanosine ("phosphate mop") to remove any residual phosphate by forming ribose 1-phosphate. The low-molecular weight species of the "P_i mop" are removed by exchanging the buffer with 50 mM Hepes (pH 7.8) and 2 mM TCEP using Amicon Ultra centrifugal filter devices (10000 molecular weight cutoff). The purity of the labeled protein was confirmed by sodium dodecyl sulfate−polyacrylamide gel electrophoresis (SDS−PAGE). The protein concentration and yield are determined by the absorbance at 280 nm using a molecular weight of 35276 and a calculated extinction coefficient of 64204 M^{-1} cm^{-1}, and protein stocks were stored at −80 °C.

Preparation of WT FTase. Recombinant rat protein FTase expression and purification were conducted in *Escherichia coli* BL21(DE3) FPT/pET23a cells as described previously.[23,35] The purified FTase was determined by SDS−PAGE to be >90% pure. The protein was dialyzed at 4 °C against 50 mM

Hepes (pH 7.8) and 2 mM TCEP and stored at −80 °C. The concentration of FTase was determined by active site titration as previously described.[23]

Single-Turnover Kinetics. The single-turnover rate constant was determined by measuring the release of diphosphate (PP_i) using a fluorescently labeled phosphate binding protein (MDCC-PBP) coupled with PP_i cleavage by inorganic pyrophosphatase (PP_iase), as described by Pais et al.[27] FTase was preincubated with FPP or an analogue for >15 min at room temperature and then rapidly mixed with a peptide solution containing MDCC-PBP and PP_iase. The following final concentrations were used: 800 nM FTase, 200 nM FPP/analogue, 25 μM peptide, 5 μM MDCC-PBP, 34 units/mL PP_iase, 50 mM Heppso (pH 7.8), 5 mM $MgCl_2$, and 2 mM TCEP. Experiments were conducted at 25 °C using a KinTek model SF-2001 stopped-flow apparatus (KinTek Corp., Austin, TX) to detect an increase in fluorescence upon binding of inorganic phosphate to MDCC-PBP (λ_{ex} = 430 nm; λ_{em} = 450 nm; Corion LL-450-F cutoff filter). The stopped-flow syringes and mixing chamber were preincubated prior to experiments in buffer containing a P_i mop [50 mM Heppso (pH 7.8), 5 mM $MgCl_2$, 2 mM TCEP, 0.5 unit/mL PNPase, and 15 μM MEG]. At least five kinetic traces were averaged, and the single-turnover rate constant (k_{obs}) was determined by fitting eq 1 to the data

$$Fl = \Delta Fl \times e^{-k_{obs}t} + Fl_{max} \quad (1)$$

where Fl is the observed fluorescence at <450 nm at time t, ΔFl is the amplitude, and Fl_{max} is the fluorescence end point. The single-turnover rate constant (k_{obs}) was derived from a reversible two-step kinetic mechanism proceeding from the E·FPP·CaaX complex shown in the dashed box in Figure 1 using eq 1.

$$k_{obs} = \frac{k_{conf}k_{chem}}{k_{conf} + k_{-conf} + k_{chem}} \quad (2)$$

Steady-State Kinetics. The steady-state kinetic parameters k_{cat}, $K_M^{isoprenoid}$, and $k_{cat}/K_M^{isoprenoid}$ were determined from the dependence of the initial velocity on the concentration of FPP or an analogue at a saturating dansylated peptide (dns-GCVLS) concentration, or k_{cat} was determined from the dependence of the initial velocity on the concentration of dns-GCVLS at a saturating isoprenoid concentration. The initial velocity was measured from the time-dependent increase in fluorescence intensity (λ_{ex} = 340 nm; λ_{em} = 520 nm) upon farnesylation of dansylated GCVLS, as described previously. Reactions were initiated by the addition of FTase (final concentration of 25 nM) to solutions containing 5 μM dns-GCVLS, varying concentrations (1−20 μM) of FPP/analogue, 50 mM Heppso (pH 7.8), 5 mM $MgCl_2$, and 2 mM TCEP at 25 °C. For measurements at a fixed isoprenoid concentration, reactions were initiated by the addition of FTase (final concentration of 25 nM) to solutions containing varying concentrations (1−10 μM) of dns-GCVLS, 20 μM isoprenoid, 50 mM Heppso (pH 7.8), 5 mM $MgCl_2$, and 2 mM TCEP at 25 °C. The fluorescence intensity over time is measured for the first 10% of the reaction, using a Polarstar Galaxy fluorescence plate reader (BMG Laboratory Technologies, Durham, NC). The initial velocity of the reaction in fluorescence units per second (R) is converted to the velocity of the product formed in micromolar per second (V) using eq 3

$$V = \frac{RP}{F_{max}} \quad (3)$$

where P is the concentration of the limiting substrate and F_{max} is the amplitude in fluorescence measured from the end point of each experiment.

The values of the steady-state kinetic parameters k_{cat}, $K_M^{isoprenoid}$, and $k_{cat}/K_M^{isoprenoid}$ were calculated from a fit of the Michaelis−Menten equation to the initial V versus [S] data.

RESULTS

Design and Synthesis of Aryl-Substituted Isoprenoid Diphosphate. FPP analogues **2**−**15** (Figure 3) were designed to probe aspects of isoprenoid C1 reactivity, the isoprene conformational rearrangement, and the steric constraints of the FTase mechanism. We had previously established that an aniline or phenoxy group is an isostere for the terminal isoprene of FPP and that a range of substituent groups are tolerated by FTase to give transferable analogues under steady-state conditions. Analogues **2**−**15** were designed to test the extent that FPP could be altered and still allow transfer catalyzed by FTase. The chemical reactivity of C1 was increased by replacing the first isoprene with a benzyl moiety in analogues **13**−**15** (Table 1 and Schemes 1 and 2). Solvolysis

Scheme 1[a]

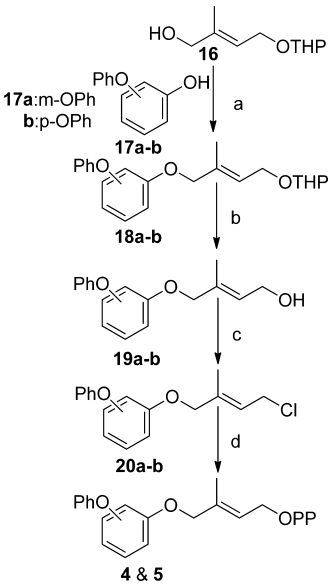

[a](a) DEAD, Ph_3P, THF; (b) PPTS, MeOH; (c) Ph_3PCl_2, CH_3CN; (d) $(n\text{-}Bu_4)_3HP_2O_7$, CH_3CN.

studies suggest benzyl isoprenoids **13**−**15** are expected to be 5 and 20 times more reactive than the corresponding allylic isoprenoids in S_N1- and S_N2-type reactions, respectively.[36,37] The terminal isoprene was replaced by an aromatic group in analogues **2**−**12** and **15** but retained in analogues **13** and **14**. The second isoprene in analogues **4**−**12** and **15** was replaced by a series of substituted phenyl groups. In analogues **4**−**12**, the first isoprene unit was retained and the steric demands and the number of rotatable bonds relative to FPP were varied. Analogue **12** is longer than the other FPP analogues and was designed to mimic the 20-carbon geranylgeranyl diphosphate (GGPP). GGPP is an alternative FTase substrate for some

dx.doi.org/10.1021/bi3011362 | Biochemistry 2012, 51, 8307−8319

Scheme 2[a]

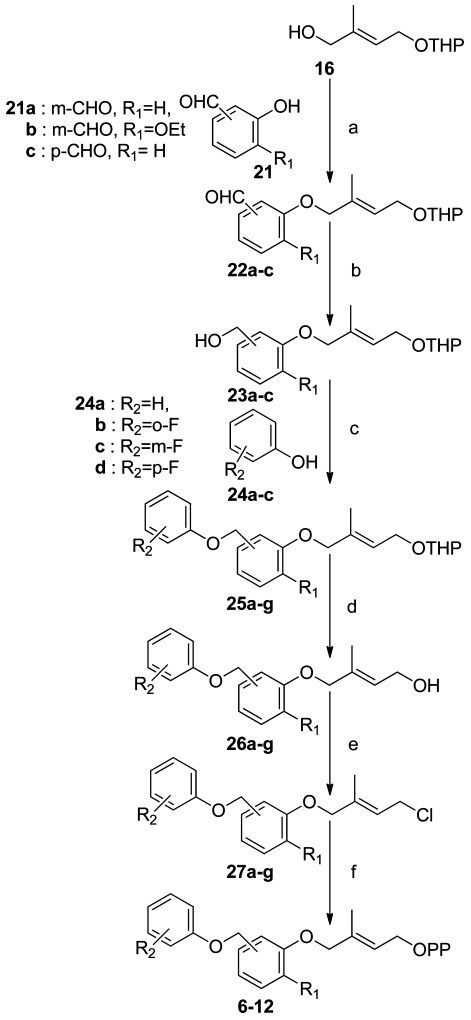

[a](a) DEAD, Ph_3P, THF; (b) $NaBH_4$, EtOH; (c) DEAD, Ph_3P, THF; (d) PPTS, MeOH; (e) Ph_3PCl_2, CH_3CN; (f) $(n\text{-}Bu_4)_3HP_2O_7$, CH_3CN.

peptide sequences but is a nanomolar inhibitor of the enzyme with others.[38−40]

Analogues **2** and **3** were prepared as previously reported.[14,41] Analogues **4** and **5** were prepared by Mitsunobu coupling of either *m*- or *p*-phenoxyphenol with alcohol **16** to give THP-protected isoprenols **18a** and **18b** (Scheme 1). Removal of the THP ether with PPTS in methanol afforded alcohols **19a** and **19b** that were converted to the corresponding chlorides **20a** and **20b**, respectively, using Ph_3PCl_2 in acetonitrile.[14] The allylic chlorides were diphosphorylated with $(n\text{-}Bu_4)_3HP_2O_7$ to give diphosphates **4** and **5** in moderate yield.

The preparation of FPP analogues **6**−**12** is shown in Scheme 2 and involved Mitsunobu coupling of alcohol **16** with the appropriate hydroxybenzaldehyde to give aldehydes **22a**−**c** that were reduced with $NaBH_4$ to the corresponding benzyl alcohols **23a**−**c**, respectively. A second Mitsunobu reaction with the requisite substituted phenols then afforded THP ethers **25a**−**g**. These protected isoprenoid analogues were converted to the desired diphosphates **6**−**12**, respectively, as described above.

Synthesis of FPP analogues **13** and **14** where the first isoprene moiety was replaced with a benzyl group is shown in Scheme 3. Mitsunobu coupling of geraniol with either *m*- or *p*-

Scheme 3[a]

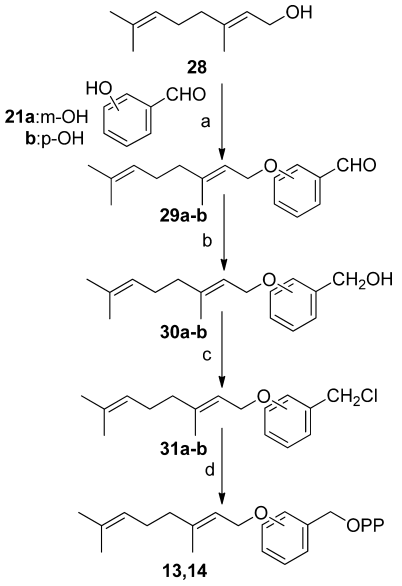

[a](a) DEAD, Ph_3P, THF; (b) $NaBH_4$, EtOH; (c) Ph_3PCl_2, CH_3CN; (d) $(n\text{-}Bu_4)_3HP_2O_7$, CH_3CN.

hydroxybenzaldehyde followed by reduction of aldehydes **29a** and **29b** with $NaBH_4$ gave the corresponding alcohols **30a** and **30b**, respectively. The desired diphosphates **13** and **14** were obtained by conversion of these alcohols as described above.

Synthesis of analogue **15** where all of the isoprene units are replaced by aromatic moieties is shown in Scheme 4. Previously described chloride **32**[42] was coupled with the sodium salt of *m*-phenoxyphenol followed by removal of the THP protecting group, chlorination, and diphosphorylation as described above.

Scheme 4[a]

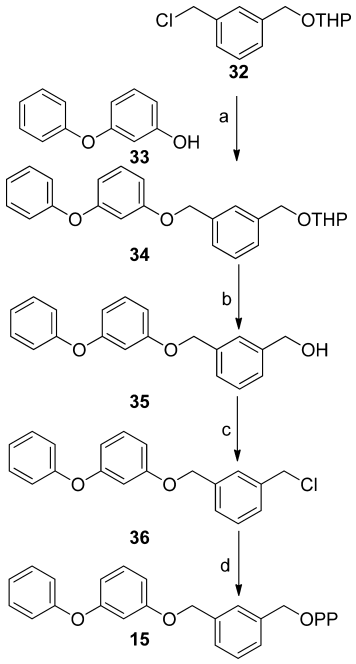

[a](a) NaH, THF; (b) PPTS, MeOH; (c) Ph_3PCl_2, CH_3CN; (d) $(n\text{-}Bu_4)_3HP_2O_7$, CH_3CN.

dx.doi.org/10.1021/bi3011362 | *Biochemistry* 2012, 51, 8307−8319

FTase-Catalyzed Alkylation of GCVLS Depends on the Isoprenoid Donor Structure. A fluorescent assay was used to determine the effect of the FPP analogue structure on multiple-turnover kinetics catalyzed by FTase. The steady-state kinetic parameters k_{cat} for **1**−**15** and $K_M^{isoprenoid}$ of FPP and analogues **2**, **3**, **6**, **7**, **9**−**11**, and **13**−**15** with dansylated GCVLS peptide (dns-GCVLS) were measured (Table 1). $K_M^{isoprenoid}$ was measured by varying the FPP or analogue concentration in the presence of a saturating peptide concentration, and k_{cat} was measured by varying the isoprenoid concentration in the presence of a saturating peptide concentration or by varying the peptide concentration in the presence of a saturating analogue concentration.[43] The dns-GCVLS peptide corresponds to the well-characterized Ca_1a_2X sequence of H-Ras.[21,39,44]

FTase catalyzed transfer of the analogues to dns-GCVLS with an efficiency equal to or lower than that of FPP, with the exception of the GGPP mimetic **12** for which no turnover was detected. For the FPP analogues in which the third isoprene is replaced with substituted aniline groups, the steady-state kinetic parameters depend in a complex manner on the size and ring position of the substituents, and the sequence of the Ca_1a_2X peptide. For example, analogue **2** is a poor donor for modification of the dansyl-GCVLS peptide but is a good substrate with the dansyl-GCVIM peptide. The steady-state rate constant $k_{cat}/K_M^{isoprenoid}$ is termed the "specificity constant" for the reaction of a peptide with different isoprenoids and can be used to determine how efficiently the FPP analogue is transferred to the peptide.[15,30,31] Relative to that of FPP, the value of $k_{cat}/K_M^{isoprenoid}$ for the analogues decreases up to 475-fold. Analysis of the steady-state parameters reveals that rate constant k_{cat} decreases for the analogues 1.3−220-fold relative to that of FPP, while the value of $K_M^{isoprenoid}$ varies from 0.2 to 9.2 μM, which is within a 7.5-fold difference of that of FPP ($K_M^{isoprenoid}$ = 1.5 μM). Therefore, the decreases in k_{cat} roughly follow the same trends observed for $k_{cat}/K_M^{isoprenoid}$.

The efficiency of the multiple-turnover reaction depends on analogue structure. Notably, a *meta* or *para* linkage geometry of the second isoprene substitution does not appear to alter the value of $k_{cat}/K_M^{isoprenoid}$ for modification of peptides catalyzed by FTase. For example, compounds **9** (*meta*) and **6** (*para*) have very similar efficiencies. Furthermore, the reactivity of analogues with dns-GCVLS does not depend on having the same number of rotatable bonds as FPP. Analogue **15** has seven rotatable bonds compared with eight in FPP. Clearly, the rotatable bonds in these analogues can adopt conformations sufficient to achieve the reactive ternary complex and the transition state. In contrast, the FTase-catalyzed efficiency of alkylation of peptides with analogues **10** and **11** is severely compromised, suggesting that increased steric bulk on the lipid reduces either the peptide affinity or the rate constant for product formation.

Analogues in Which the α-Isoprene Is Replaced with a Benzyl Group Can Be Transferred by FTase. Benzyl analogues **13**−**15** are surprisingly good substrates, with $k_{cat}/K_M^{isoprenoid}$ values that are within a factor of 3 of that of FPP (Table 1). Remarkably, analogue **15** is almost as good a substrate as FPP for FTase despite having no isoprene units in the structure. Aryl analogue **13** shows that most of the reactivity of FPP is retained by substituting a benzyl group for the first isoprene. This is the first time FTase has been shown to catalyze the transfer of an isoprenoid with a non-allylic diphosphate to a Ca_1a_2X peptide.

The Single-Turnover Rate Constant for GCVLS Alkylation Is the Same for Structurally Divergent Isoprenoid Diphosphates. We measured the STO rate constant (k_{obs}) for FTase-catalyzed alkylation of GCVLS by FPP and analogues **2**−**15** using a fluorescence-based assay that detects the release of pyrophosphate following alkyl transfer under conditions of excess FTase and peptide and limiting isoprenoid diphosphate analogue.[45] The observed rate constant for alkylated peptide product formation (k_{obs}), indicated in Figure 1, measures formation of the E·product complex from the ternary E·FPP·peptide complex and includes both the chemical farnesylation step (k_{chem}) and the proposed FPP rotational rearrangement (k_{conf}) to form the active substrate conformation (eq 3).[26,27,31] Surprisingly, the observed rate constant under STO conditions (k_{obs}) for all of the analogues is very similar to that measured for FPP (Table 1). The discrepancy between the effects of these analogues on the single-turnover and steady-state kinetics suggests that different rate-limiting steps are being measured by the two methods; in particular, product dissociation may contribute significantly to the measured values for the steady-state kinetics.

The Rate Constant for Alkylation Depends on the Ca_1a_2X Peptide Sequence. To delineate the dependence of the STO rate constants on peptide structure, we also measured the reactivity of analogues **2**−**15** for TKCVIM and TKCVIF (Table 1). TKCVIM is the K-Ras Ca_1a_2X peptide, and the STO rate constant for farnesylation is nearly 2 times greater (FPP; k_{obs} = 6.5 s^{-1}) than the value for GCVLS (FPP; k_{obs} = 3.4 s^{-1}). These rate constants are in good agreement with those previously reported.[31,46] TKCVIF is the Ca_1a_2X peptide from TC21 and is normally a substrate for both FTase and GGTase I. The STO rate constant for farnesylation of TKCVIF catalyzed by FTase is 25-fold lower (FPP; k_{obs} = 0.27 s^{-1}) than the value for TKCVIM. Once again, the STO rate constants for the structurally dissimilar analogues **2**−**15** were identical to that of FPP for each of the three peptides examined (Table 1). Notably, GGPP mimetic **12** reacts as efficiently as FPP with all three peptides even though modification by this analogue under steady-state turnover conditions is undetectable. These results indicate that the conformational rearrangement and the farnesylation step are insensitive to the structural differences between FPP and analogues **2**−**15** (Table 1). Rather, the STO rate constant for peptide alkylation depends on the structure of the peptide, particularly the C-terminal residue in the Ca_1a_2X motif. The uniformly high reactivity of FPP and analogues **2**−**15** suggests a facile conformational change in the analogue hydrocarbon chains to achieve the transition state, consistent with recent computational studies.[28] Furthermore, the conformational rearrangement of the isoprenoid diphosphate in the active site to achieve the reactive conformation is independent of the product release step.

DISCUSSION

Increased Isoprenoid Chemical Reactivity Does Not Alter the Rate Constant for Peptide Alkylation. The electronic structure of the first isoprene unit is thought to be critical for the FTase-catalyzed transfer to the peptide. 3-Vinyl-FPP is an efficient alternative substrate for FTase and is likely to have an increased level of delocalization of any cationic character in the transition state.[47,48] The structure of the first isoprenoid is also an important factor in efficient multiple turnovers as both the 2*Z* isomer of FPP and 3-allyl-FPP are potent inhibitors of FTase, although they are electronically

dx.doi.org/10.1021/bi3011362 | *Biochemistry* 2012, 51, 8307−8319

almost identical to FPP. It is unknown whether these two molecules alkylate peptide substrates under STO conditions.[47,48] The reactivity of C1 in benzyl analogues **13**−**15** is increased relative to that of FPP. The solvolytic reactivity of *p*-geranyloxybenzyl diphosphate **13** is higher than that of *meta*-substituted **14** and **15** because of enhanced stabilization of the delocalized positive charge that develops on the aromatic ring in the transition state (Figure 2B).[37] The identical STO reactivity for analogues **13**−**15** indicates that enhanced stabilization of the carbocationic aspects of the transition state does not contribute to an increased observed rate constant for peptide alkylation catalyzed by FTase. These results contrast with the substantial decrease in reactivity caused by electron withdrawing fluorine substitution at the C3 methyl of FPP on both steady-state turnover and k_{chem}.[26,27]

Isoprenoid hydrophobicity is uncorrelated with efficiency in multiturnover reactions,[14] although hydrophobicity of the peptide substrates affects reactivity.[31,46] The lack of any isoprenoid structural effect for analogues **2**−**15** on the STO rates suggests that interactions between the isoprenoid and the amino acid residues lining the walls of the active site are not particularly sensitive to the polarity of the chain.

Reaction Steps Involved in FTase Isoprenoid Diphosphate Selectivity. For FTase, the steady-state parameter $k_{cat}/K_M^{isoprenoid}$ normally includes the rate constants for reaction steps for formation of the E·FPP·Ca_1a_2X complex, including peptide binding to E·FPP, and the first irreversible step of diphosphate dissociation (Figure 1).[30,31,45] However, because FPP also enhances product dissociation, the measured value of $k_{cat}/K_M^{isoprenoid}$ likely includes these steps, as well.[29] In contrast, peptide alkylation catalyzed by FTase under single-turnover conditions (with a saturating enzyme concentration) monitors only steps that occur after peptide binding through diphosphate release [k_{obs} (dashed box, Figure 1)].[45] Therefore, FTase-catalyzed single-turnover kinetics in the presence of a limiting amount of isoprenoid diphosphate isolates the alkyl transfer step (k_{chem}) and presumed isoprenoid conformational change (k_{conf}) from the dissociation of the alkylated peptide [k_{off}^{CaaX} (Figure 1)] that is frequently the rate-limiting step for k_{cat} under multiple-turnover conditions.[18,26,49] The lack of any isoprenoid structural effect, yet a strong Ca_1a_2X peptide sequence effect, on k_{obs} suggests that the chemical step and/or the proposed conformational rearrangement of the FPP depends on how the Ca_1a_2X peptide binds to FTase. The clear differences in k_{obs} for the three peptides suggest that subtle differences in the Ca_1a_2X−FTase binding interactions alter the rate of the proposed isoprenoid conformational rearrangement or alter the chemical reactivity of the thiolate nucleophile.

Increased Isoprenoid Bulk Does Not Alter the Rate Constant for GCVLS Alkylation. Previous measurements demonstrated that the secondary kinetic isotope effect (KIE) for the reaction of FPP with peptides under STO conditions catalyzed by FTase varies with the structure of the peptide; the α secondary ^{3}H KIE observed for TKCVIF is large (1.13 ± 0.01) but decreases to near unity for GCVLS.[27] The original interpretation of this result was that the conformational change became the rate-limiting step for farnesylation of GCVLS under STO conditions. However, recent computational studies from the Merz group suggest that the $\Delta G^{\ddagger}$ for the conformational step is much smaller than that of the alkylation step, even for GCVLS, and that the change in the secondary KIE reflects alterations in the transition-state structure due to changes in the peptide binding mode. The similar STO k_{obs} for all of the analogues indicates that substantial conformational freedom to achieve the transition state is available to the lipid in the confines of the active site and that any barriers to achieving the transition state are small. These observations indicate that the decreased steady-state turnover rate for the analogues most likely reflects alterations in the product dissociation step.

The Isoprenoid Structure Mainly Affects Product Release. The decoupling of isoprenoid structure and intrinsic chemical reactivity from the STO rate constant k_{obs}, while retaining a profound isoprenoid structural dependence on the rate of product release, k_{cat}, indicates that the alkylation reaction depends mainly on the structure of the peptide,[46] while product release depends on the structure of both the peptide and the isoprenoid.[30,31] Equation 2 demonstrates the contribution of conformational rearrangement k_{conf} and chemical step k_{chem} to STO rate constant k_{obs}. Inspection of eq 2 suggests that either k_{conf} and k_{-conf} are unchanged by the range of structural modifications explored here or k_{chem} is sufficiently small to be the rate-determining step for all of the substrates. This latter conclusion is consistent with computational studies suggesting that the barrier to achieving the transition state going from the E·FPP·Ca_1a_2X complex to the E·FPP·Ca_1a_2X* complex is on the order of 1 kcal/mol for CVIM to 2.5 kcal/mol for CVLM compared to ∼20 kcal/mol for the chemical step.[24,28,50]

Mg^{2+} binding accelerates FTase-catalyzed alkylation of GCVLS and TKCVIF by FPP by 700- and 100-fold, respectively. The Mg^{2+} cofactor may stabilize both the active substrate conformation and the developing charge on the pyrophosphate leaving group.[51−53] The FPP pyrophosphate leaving group in the inactive (E·FPP·Ca_1a_2X) complex is bound in the FTase PP_i binding pocket comprised of positively charged residues.[19,22,54−57] Conformational rearrangement of the FPP isoprenoid chain moves the pyrophosphate leaving group out of the PP_i binding pocket and creates a Mg^{2+} binding site that stabilizes the active complex (E·FPP·Ca_1a_2X*), which is then followed by the attack of the zinc-bound thiolate nucleophile on C1. For each CaaX peptide, the observed rate constant, k_{obs}, for analogues **2**−**15** were identical to that of the natural substrate FPP. The insensitivity of k_{obs} to the increased chemical reactivity of analogues **13**−**15** indicates that the rate of chemical step k_{chem} for each of the three peptides was not limited by the intrinsic reactivity of the allylic C1 electrophile. Furthermore, the insensitivity of k_{obs} to the structure of the analogues for all three peptides suggests that there is abundant room in the active site for the proposed conformational rearrangement of the isoprenoid to take place. Consistent with this model, the uniform observed values of k_{obs} for FPP and analogues **2**−**15** could be accommodated by correlated changes in chemical reactivity that compensate for an isoprenoid structure-dependent decrease in the ratio of the equilibrium constant for the conformational change (k_{conf}/k_{-conf}). However, there is no increase in k_{obs} relative to that of FPP for the more reactive benzyl analogues **13**−**15**, suggesting that k_{chem} depends on the CaaX peptide sequence and does not vary with isoprenoid structure.

Implications for the Development of Alternative FTase Substrates That Block Prenylated Protein Function (PFIs). This study tested the sensitivity of the chemical step to changes in the electronic structure of the lipid electrophile and the sensitivity of the conformational rearrangement required to achieve the reactive conformation to changes in the lipid structure. There are four primary conclusions. (1) Increases in the chemical reactivity of the lipid electrophile do

not increase k_{obs}, and (2) increased steric bulk in the isoprene chain does not decrease k_{obs}. (3) k_{obs} depends on the Ca_1a_2X X-residue, and (4) in contrast, the steady-state rate constants for turnover are highly dependent on lipid structure. The ability of FTase to transfer analogues with no isoprene units opens the door to a much wider range of alternative structures as potential PFIs. These results suggest that as long as the chemical reactivity of the analogue C1 is at least as reactive as the allylic group of FPP, efficient S-alkylation is possible and largely unaffected by the chemical structure and bulk of the isoprenoid chain. There must be limits to the size of transferrable lipid moieties, as the FTase pocket has finite dimensions. However, the limits were not reached by the analogues investigated in this study. In contrast to the structure-independent rate of cysteine alkylation, product release was highly dependent on the structure of the analogue. Previously, our lab and others have noted a Ca_1a_2X sequence-dependent interplay in the turnover of FPP analogues.[30,32] Despite investigation of almost 200 analogues with a wide range of chemical structures, no clear structure−activity relationship has emerged. Broadly, large analogues like **10**−**12** are inefficiently turned over. Furthermore, these data suggest that the farnesyl binding site in the exit groove may be significantly more selective for the farnesyl diphosphate substrate than the active site binding pocket and therefore might be a useful site for the design of novel inhibitors. Alternatively, the conformation of the isoprenoid in the E·product complex may block efficient binding of the new analogue diphosphate in the exit groove or is inhibited from rearranging to put the alkylated isoprenoid into the exit groove.

■ ASSOCIATED CONTENT

Supporting Information

Detailed experimental procedure for the synthesis of all new compounds; ^{1}H NMR spectra of **19a**, **19b**, **26a**−**g**, **30a**, **30b**, and **35**; and ^{1}H, ^{13}P, and LR mass spectra of **3**−**15**. This material is available free of charge via the Internet at http://pubs.acs.org.

■ AUTHOR INFORMATION

Corresponding Author

*E-mail: hps@uky.edu.

Present Addresses

[‖]Department of Biochemistry, University of Wisconsin, 433 Babcock Dr., Madison, WI 53706.

[⊥]Immunology Institute, Shandong University School of Medicine, Jinan, Shandong, People's Republic of China.

[@]Chemistry Department, University of North Carolina, 9201 University City Blvd., Charlotte, NC 28223-0001.

Funding

Supported by National Institutes of Health Grants R01 GM66152 to H.P.S. and R01 GM40602 to C.A.F.

Notes

The authors declare no competing financial interest.

■ ABBREVIATIONS

FTase, farnesyltransferase; AGPP, 8-anilinogeranyl diphosphate; FPP, farnesyl diphosphate; TLC, thin layer chromatography; GGTase I, geranylgeranyl transferase; FTI, farnesyltransferase; Ca_1a_2X, tetrapeptide sequence cysteine aliphatic amino acid-aliphatic amino acid-X (serine, glutamine, or methionine); GGPP, geranylgeranyl diphosphate; DEAD, diethylazodicarboxylate; DMF, dimethylformamide; THF, tetrahydrofuran; PPTS, pyridinium-*p*-toluene sulfonate; H-Ras, Harvey-Ras; K-Ras, Kirsten-Ras; DTT, dithiothreitol; RP-HPLC, reverse phase high-performance liquid chromatography; PBP, phosphate binding protein; k_{cat}, turnover number; $K_M^{isoprenoid}$, Michaelis−Menten constant for FPP or an analogue; MDCC, diethylamino-3-[*N*-(2-maleimidoethyl)-carbamoyl]coumarin; PNPase, polynucleotide phosphorylase; TCEP, tris(2-carboxyethyl)phosphine hydrochloride.

■ REFERENCES

(1) Fu, H. W., and Casey, P. J. (1999) Enzymology and biology of CaaX protein prenylation. *Recent Prog. Horm. Res. 54*, 315−342.

(2) Casey, P. J., and Seabra, M. C. (1996) Protein prenyltransferases. *J. Biol. Chem. 271*, 5289−5292.

(3) Adjei, A. A. (2003) An overview of farnesyltransferase inhibitors and their role in lung cancer therapy. *Lung Cancer 41* (Suppl. 1), S55−S62.

(4) Rowinsky, E. K., Windle, J. J., and Von Hoff, D. D. (1999) Ras protein farnesyltransferase: A strategic target for anticancer therapeutic development. *J. Clin. Oncol. 17*, 3631−3652.

(5) Zhang, F. L., and Casey, P. J. (1996) Influence of metal ions on substrate binding and catalytic activity of mammalian protein geranylgeranyltransferase type-I. *Biochem. J. 320* (Part 3), 925−932.

(6) Sousa, S. F., Fernandes, P. A., and Ramos, M. J. (2005) Unraveling the mechanism of the farnesyltransferase enzyme. *J. Biol. Inorg. Chem. 10*, 3−10.

(7) Vergnes, L., Peterfy, M., Bergo, M. O., Young, S. G., and Reue, K. (2004) Lamin B1 is required for mouse development and nuclear integrity. *Proc. Natl. Acad. Sci. U.S.A. 101*, 10428−10433.

(8) Konstantinopoulos, P. A., Karamouzis, M. V., and Papavassiliou, A. G. (2007) Post-translational modifications and regulation of the RAS superfamily of GTPases as anticancer targets. *Nat. Rev. Drug Discovery 6*, 541−555.

(9) Reents, R., Wagner, M., Schlummer, S., Kuhlmann, J., and Waldmann, H. (2005) Synthesis and application of fluorescent ras proteins for live-cell imaging. *ChemBioChem 6*, 86−94.

(10) Rando, R. R. (1996) Chemical biology of isoprenylation/methylation. *Biochem. Soc. Trans. 24*, 682−687.

(11) Figueroa, C., Taylor, J., and Vojtek, A. B. (2001) Prenylated Rab acceptor protein is a receptor for prenylated small GTPases. *J. Biol. Chem. 276*, 28219−28225.

(12) Whyte, D. B., Kirschmeier, P., Hockenberry, T. N., Nunez-Oliva, I., James, L., Catino, J. J., Bishop, W. R., and Pai, J. K. (1997) K- and N-Ras are geranylgeranylated in cells treated with farnesyl protein transferase inhibitors. *J. Biol. Chem. 272*, 14459−14464.

(13) Roberts, M. J., Troutman, J. M., Chehade, K. A., Cha, H. C., Kao, J. P., Huang, X., Zhan, C. G., Peterson, Y. K., Subramanian, T., Kamalakkannan, S., Andres, D. A., and Spielmann, H. P. (2006) Hydrophilic anilinogeranyl diphosphate prenyl analogues are Ras function inhibitors. *Biochemistry 45*, 15862−15872.

(14) Subramanian, T., Liu, S., Troutman, J. M., Andres, D. A., and Spielmann, H. P. (2008) Protein farnesyltransferase-catalyzed isoprenoid transfer to peptide depends on lipid size and shape, not hydrophobicity. *ChemBioChem 9*, 2872−2882.

(15) Troutman, J. M., Subramanian, T., Andres, D. A., and Spielmann, H. P. (2007) Selective modification of CaaX peptides with ortho-substituted anilinogeranyl lipids by protein farnesyl transferase: Competitive substrates and potent inhibitors from a library of farnesyl diphosphate analogues. *Biochemistry 46*, 11310−11321.

(16) Placzek, A. T., Hougland, J. L., and Gibbs, R. A. (2012) Synthesis of frame-shifted farnesyl diphosphate analogs. *Org. Lett. 14*, 4038−4041.

(17) Nguyen, U. T., Goody, R. S., and Alexandrov, K. (2010) Understanding and exploiting protein prenyltransferases. *ChemBioChem 11*, 1194−1201.

(18) Furfine, E. S., Leban, J. J., Landavazo, A., Moomaw, J. F., and Casey, P. J. (1995) Protein farnesyltransferase: Kinetics of farnesyl pyrophosphate binding and product release. *Biochemistry 34*, 6857–6862.
(19) Long, S. B., Casey, P. J., and Beese, L. S. (1998) Cocrystal structure of protein farnesyltransferase complexed with a farnesyl diphosphate substrate. *Biochemistry 37*, 9612–9618.
(20) Huang, C. C., Casey, P. J., and Fierke, C. A. (1997) Evidence for a catalytic role of zinc in protein farnesyltransferase. Spectroscopy of Co^{2+}-farnesyltransferase indicates metal coordination of the substrate thiolate. *J. Biol. Chem. 272*, 20–23.
(21) Pompliano, D. L., Rands, E., Schaber, M. D., Mosser, S. D., Anthony, N. J., and Gibbs, J. B. (1992) Steady-state kinetic mechanism of Ras farnesyl:protein transferase. *Biochemistry 31*, 3800–3807.
(22) Long, S. B., Casey, P. J., and Beese, L. S. (2002) Reaction path of protein farnesyltransferase at atomic resolution. *Nature 419*, 645–650.
(23) Bowers, K. E., and Fierke, C. A. (2004) Positively charged side chains in protein farnesyltransferase enhance catalysis by stabilizing the formation of the diphosphate leaving group. *Biochemistry 43*, 5256–5265.
(24) Cui, G., and Merz, K. M., Jr. (2007) Computational studies of the farnesyltransferase ternary complex part II: The conformational activation of farnesyldiphosphate. *Biochemistry 46*, 12375–12381.
(25) Dolence, J. M., and Poulter, C. D. (1995) A mechanism for posttranslational modifications of proteins by yeast protein farnesyltransferase. *Proc. Natl. Acad. Sci. U.S.A. 92*, 5008–5011.
(26) Huang, C., Hightower, K. E., and Fierke, C. A. (2000) Mechanistic studies of rat protein farnesyltransferase indicate an associative transition state. *Biochemistry 39*, 2593–2602.
(27) Pais, J. E., Bowers, K. E., and Fierke, C. A. (2006) Measurement of the α-secondary kinetic isotope effect for the reaction catalyzed by mammalian protein farnesyltransferase. *J. Am. Chem. Soc. 128*, 15086–15087.
(28) Yang, Y., Wang, B., Ucisik, M. N., Cui, G., Fierke, C. A., and Merz, K. M., Jr. (2012) Insights into the mechanistic dichotomy of the protein farnesyltransferase peptide substrates CVIM and CVLS. *J. Am. Chem. Soc. 134*, 820–823.
(29) Tschantz, W. R., Furfine, E. S., and Casey, P. J. (1997) Substrate binding is required for release of product from mammalian protein farnesyltransferase. *J. Biol. Chem. 272*, 9989–9993.
(30) Troutman, J. M., Andres, D. A., and Spielmann, H. P. (2007) Protein farnesyl transferase target selectivity is dependent upon peptide stimulated product release. *Biochemistry 46*, 11299–11309.
(31) Hougland, J. L., Lamphear, C. L., Scott, S. A., Gibbs, R. A., and Fierke, C. A. (2009) Context-dependent substrate recognition by protein farnesyltransferase. *Biochemistry 48*, 1691–1701.
(32) Reigard, S. A., Zahn, T. J., Haworth, K. B., Hicks, K. A., Fierke, C. A., and Gibbs, R. A. (2005) Interplay of isoprenoid and peptide substrate specificity in protein farnesyltransferase. *Biochemistry 44*, 11214–11223.
(33) Krzysiak, A. J., Aditya, A. V., Hougland, J. L., Fierke, C. A., and Gibbs, R. A. (2010) Synthesis and screening of a CaaL peptide library versus FTase reveals a surprising number of substrates. *Bioorg. Med. Chem. Lett. 20*, 767–770.
(34) Hirshberg, M., Henrick, K., Haire, L. L., Vasisht, N., Brune, M., Corrie, J. E., and Webb, M. R. (1998) Crystal structure of phosphate binding protein labeled with a coumarin fluorophore, a probe for inorganic phosphate. *Biochemistry 37*, 10381–10385.
(35) Zimmerman, K. K., Scholten, J. D., Huang, C. C., Fierke, C. A., and Hupe, D. J. (1998) High-level expression of rat farnesyl:protein transferase in *Escherichia coli* as a translationally coupled heterodimer. *Protein Expression Purif. 14*, 395–402.
(36) Mu, Y. Q., Omer, C. A., and Gibbs, R. A. (1996) On the stereochemical course of human protein-farnesyl transferase. *J. Am. Chem. Soc. 118*, 1817–1823.
(37) March, J. (1968) *Advanced Organic Chemistry*, 2nd ed., McGraw-Hill, New York.
(38) Shao, Y., Eummer, J. T., and Gibbs, R. A. (1999) Stereospecific synthesis and biological evaluation of farnesyl diphosphate isomers. *Org. Lett. 1*, 627–630.
(39) Chehade, K. A., Kiegiel, K., Isaacs, R. J., Pickett, J. S., Bowers, K. E., Fierke, C. A., Andres, D. A., and Spielmann, H. P. (2002) Photoaffinity analogues of farnesyl pyrophosphate transferable by protein farnesyl transferase. *J. Am. Chem. Soc. 124*, 8206–8219.
(40) Henriksen, B. S., Zahn, T. J., Evanseck, J. D., Firestine, S. M., and Gibbs, R. A. (2005) Computational and conformational evaluation of FTase alternative substrates: Insight into a novel enzyme binding pocket. *J. Chem. Inf. Model. 45*, 1047–1052.
(41) Chehade, K. A., Andres, D. A., Morimoto, H., and Spielmann, H. P. (2000) Design and synthesis of a transferable farnesyl pyrophosphate analogue to Ras by protein farnesyltransferase. *J. Org. Chem. 65*, 3027–3033.
(42) Naghipour, A., Sabounchei, S. J., Morales-Morales, D., Hernandez-Ortega, S., and Jensen, C. M. (2004) Synthesis of a new class of unsymmetrical PCP′ pincer ligands and their palladium(II) complexes: X-ray structure determination of $PdCl\{C_6H_3$-2-CH_2PPh_2-6-$CH_2PBu_2t\}$. *J. Organomet. Chem. 689*, 2494–2502.
(43) Micali, E., Chehade, K. A., Isaacs, R. J., Andres, D. A., and Spielmann, H. P. (2001) Protein farnesyltransferase isoprenoid substrate discrimination is dependent on isoprene double bonds and branched methyl groups. *Biochemistry 40*, 12254–12265.
(44) Cassidy, P. B., Dolence, J. M., and Poulter, C. D. (1995) Continuous fluorescence assay for protein prenyltransferases. *Methods Enzymol. 250*, 30–43.
(45) Pais, J. E., Bowers, K. E., Stoddard, A. K., and Fierke, C. A. (2005) A continuous fluorescent assay for protein prenyltransferases measuring diphosphate release. *Anal. Biochem. 345*, 302–311.
(46) Hartman, H. L., Hicks, K. A., and Fierke, C. A. (2005) Peptide specificity of protein prenyltransferases is determined mainly by reactivity rather than binding affinity. *Biochemistry 44*, 15314–15324.
(47) Zahn, T. J., Whitney, J., Weinbaum, C., and Gibbs, R. A. (2001) Synthesis and evaluation of GGPP geometric isomers: Divergent substrate specificities of FTase and GGTase I. *Bioorg. Med. Chem. Lett. 11*, 1605–1608.
(48) Rawat, D. S., Krzysiak, A. J., and Gibbs, R. A. (2008) Synthesis and biochemical evaluation of 3,7-disubstituted farnesyl diphosphate analogues. *J. Org. Chem. 73*, 1881–1887.
(49) Mathis, J. R., and Poulter, C. D. (1997) Yeast protein farnesyltransferase: A pre-steady-state kinetic analysis. *Biochemistry 36*, 6367–6376.
(50) Cui, G., Wang, B., and Merz, K. M., Jr. (2005) Computational studies of the farnesyltransferase ternary complex part I: Substrate binding. *Biochemistry 44*, 16513–16523.
(51) Pickett, J. S., Bowers, K. E., and Fierke, C. A. (2003) Mutagenesis studies of protein farnesyltransferase implicate aspartate β352 as a magnesium ligand. *J. Biol. Chem. 278*, 51243–51250.
(52) Pickett, J. S., Bowers, K. E., Hartman, H. L., Fu, H. W., Embry, A. C., Casey, P. J., and Fierke, C. A. (2003) Kinetic studies of protein farnesyltransferase mutants establish active substrate conformation. *Biochemistry 42*, 9741–9748.
(53) Saderholm, M. J., Hightower, K. E., and Fierke, C. A. (2000) Role of metals in the reaction catalyzed by protein farnesyltransferase. *Biochemistry 39*, 12398–12405.
(54) Long, S. B., Hancock, P. J., Kral, A. M., Hellinga, H. W., and Beese, L. S. (2001) The crystal structure of human protein farnesyltransferase reveals the basis for inhibition by CaaX tetrapeptides and their mimetics. *Proc. Natl. Acad. Sci. U.S.A. 98*, 12948–12953.
(55) Park, H. W., Boduluri, S. R., Moomaw, J. F., Casey, P. J., and Beese, L. S. (1997) Crystal structure of protein farnesyltransferase at 2.25 angstrom resolution. *Science 275*, 1800–1804.
(56) Reid, T. S., Terry, K. L., Casey, P. J., and Beese, L. S. (2004) Crystallographic analysis of CaaX prenyltransferases complexed with substrates defines rules of protein substrate selectivity. *J. Mol. Biol. 343*, 417–433.

(57) Strickland, C. L., Windsor, W. T., Syto, R., Wang, L., Bond, R., Wu, Z., Schwartz, J., Le, H. V., Beese, L. S., and Weber, P. C. (1998) Crystal structure of farnesyl protein transferase complexed with a CaaX peptide and farnesyl diphosphate analogue. *Biochemistry 37*, 16601−16611.
(58) Hougland, J. L., and Fierke, C. A. (2009) Getting a handle on protein prenylation. *Nat. Chem. Biol. 5*, 197−198.